JOURNAL OF MATERIALS PROCESSING TECHNOLOGY 208 (2008) 14–23

journal homepage: www.elsevier.com/locate/jmatprotec

Correlation of grinding wheel topography and grinding performance: A study from a viewpoint of three-dimensional surface characterisation

Anh Tuan Nguyen[a,*], *David Lee Butler*[b]

[a] *Department of Industrial Systems Engineering, Faculty of Mechanical Engineering, Ho Chi Minh City University of Technology, Viet Nam*
[b] *School of Mechanical and Aerospace Engineering, Nanyang Technological University, Singapore 639798, Singapore*

ARTICLE INFO

Article history:
Received 22 December 2004
Received in revised form
10 January 2007
Accepted 27 December 2007

Keywords:
Grinding
Wheel topography
Surface characterisation

ABSTRACT

Grinding wheel topography and its grinding performance was studied using an experiment, in which the truing operations were varied according to a factorial design. The correlation of wheel topography and its performance is characterised through the employment of three-dimensional surface characterisation parameters. The density of summits S_{ds}, the summits curvature S_{sc}, and the root-mean-square roughness S_q are used to characterise the density of abrasive grains, the sharpness of abrasive grains, and the coarseness of the wheel, respectively. A new criterion for selecting the optimal sampling interval ($S_{al}/4 \leq \Delta \leq S_{al}/3$) is also proposed.

1. Introduction

Grinding is a complex manufacturing process, influenced by factors such as wheel, workpiece, machine, and process setting. Among the factors, the grinding wheel is a unique one, differentiating the grinding process from other machining techniques. It is a well-known fact that the wheel topography and the conditions under which it is prepared have a profound influence upon the grinding performance – as evidenced by the grinding forces, power consumption, cutting zone temperatures, and also the surface finish of the workpiece. Thus, it is not surprising that the correlation of wheel topography and its performance has been extensively studied in the past decades (Malkin, 1998).

The question that often arises in studying the grinding wheel is how to express the topographical characteristics of grinding wheels as well as the effect of wheel topography on the process. As the abrasive grains are geometrically undefined in shape as well as location, it is often necessary to describe the cutting capability with statistical parameters. On one hand, the defined parameters should present the intrinsic characteristic of the grinding wheel; on the other, they should correlate with the wheel performance.

Grinding wheels are often characterised by the density of abrasive grains and cutting edges. Verkerk (1977) differentiated the static grains and cutting edges, which are present in the wheel surface, from the dynamic ones, which are those actually taking part in the material removal process. Although the concept is simple, the determination of the static and dynamic grains is complicated with highly inconsistent results (Verkerk, 1977).

Alternatively, the fractal dimension has been used for the characterisation of grinding wheels (Liao, 1995; Higuchi et al., 1994). Liao (1995) found the correlation between the fractal

* *Corresponding author*. Tel.: +84 8 8649300; fax: +84 8 8653823.
E-mail address: ntanh@hcmut.edu.vn (A.T. Nguyen).
0924-0136/$ – see front matter © 2008 Elsevier B.V. All rights reserved.
doi:10.1016/j.jmatprotec.2007.12.128

dimension of the wheel profiles and the surface finish of the workpiece as well as the grinding forces, in which the grinding wheels with large fractal dimension produce smaller grinding forces and smoother finish. Nakajima (1978) characterised the performance of the grinding wheel with a grindactivity coefficient, estimated as a function of infeed rate of wheel head, spark-in time and the wheel wear rate. Brinksmeier and Cinar (1995) characterised the dressing operation by using the collision number of the abrasive grain. They concluded that the active surface topography of the grinding wheel after dressing was strongly correlated with the collision number. Tonshoff et al. (1998) showed that the bearing ratio curve of the grinding wheel was affected by wheel wear.

This paper studies the application of three-dimensional (3D) surface parameters in grinding process characterisation through the employment of a factorial experiment. The 3D parameters employed were first proposed by Stout et al. (1993) as part of a European Project aimed at developing a framework for 3D topographic measurement and characterisation. Several of these parameters will be selected and will be shown to correlate with experimental grinding results. The paper will also demonstrate the influence of the sampling conditions on the parametric results before concluding.

2. Three-dimensional characterisation of grinding wheels

The measurement of surfaces in three dimensions has only really become available to the general user in the last 15 years (Stout et al., 1993). Three-dimensional measurement possesses several advantages over the more commonly accepted profilometry methods, these include the reduction in influence of erroneous features, statistically more meaningful, and the facility to analyse the structural function of the surface. Recently, preliminary studies of the three-dimensional parameters revealed that they could be used to characterise the grinding wheel topography. Blunt and Ebdon (1996) showed that by appropriate choosing the sampling conditions, the 3D parameter density of summits can be used as the density of static abrasive grains. Butler et al. (2002) demonstrated the correlation of some 3D parameters of the grinding wheel with the grinding performance.

For the work described in this paper, three of the parameters, namely, density of summits S_{ds}, summit curvature S_{sc}, and root-mean-square roughness S_q, were selected. The density of summits parameter S_{ds}, which is the 3D counterpart of the 2D peak count (ASME, 1995), is used as the density of the static abrasive grains. S_{ds} is defined by the following equation:

$$S_{ds} = \frac{\text{number of summits}}{(M-1)(N-1)\Delta x \Delta y} \quad (1)$$

where M and N are the number of data points in x and y directions; Δx and Δy are the sampling interval in x and y directions. However, before S_{ds} can be employed, it is necessary to define a summit—the usual definition being a high point surrounded by 8 lower lying points.

The summits curvature parameter S_{sc}, calculation of which involves the radius of the summit, would present the sharpness of summits. Sharper summit would generate a larger S_{sc}

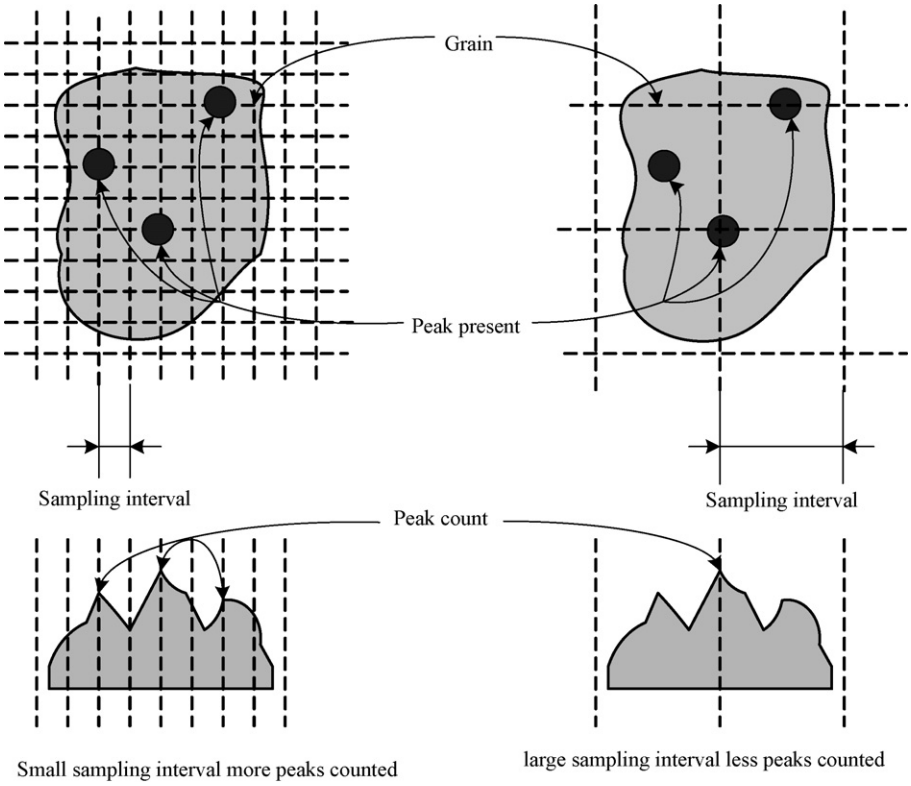

Fig. 1 – The effect of sampling intervals on counting abrasive grains.

value and vice versa. S_{sc} is estimated as follows:

$$S_{sc} = -\frac{1}{2n}\sum_{k=1}^{n}\left(\frac{\partial\eta^2(x,y)}{\partial x^2} + \frac{\partial\eta^2(x,y)}{\partial y^2}\right) \quad (2)$$

where $\eta(x, y)$ is the surface height from the reference plane.

The root-mean-square roughness S_q, which is the 3D equivalent of R_q (ASME, 1995), is used to describe the coarseness of the surface. The following equation is used to estimate S_q:

$$S_q = \sqrt{\frac{1}{MN}\sum_{j=1}^{N}\sum_{i=1}^{M}|\eta^2(x_i, y_j)|} \quad (3)$$

3. Measurement strategy

Spatial parameters S_{ds} and S_{sc}, however, should be used with caution owing to its dependence on the sampling interval. With a smaller sampling interval, a larger number of peaks will be counted (Fig. 1). As an abrasive grain will likely have more than one peak, it is crucial to select a correct interval so that a grain is counted. In order to use S_{ds} as measure of the number of abrasive grains, Blunt and Ebdon (1996) proposed that the optimum sampling interval is

$$\frac{d_g}{4} \le \Delta \le \frac{d_g}{3} \quad (4)$$

where d_g is the mean diameter of the grains. The use of the average diameter however has limitation, as it does not account for the varied distribution and size of the abrasive grains in the grinding wheel. The actual grain distribution and size may vary considerably within a given wheel owing to non-uniform packing, grain shapes, the effect of dressing operation, and wear.

To account for such a variation, we propose the use of the correlation length S_{al} as a criterion for counting the number of abrasive grains. S_{al} is defined as the horizontal distance of the autocorrelation function, which has the fastest decay to 0.2, and is estimated as follows:

$$S_{al} = \min\left(\sqrt{\tau_x^2 + \tau_y^2}\right), \qquad R(\tau_x, \tau_y) \le 0.2 \quad (5)$$

where τ_x and τ_y are the lag distances in the x and y directions; $R(\tau_x, \tau_y)$ is the autocorrelation function.

Fig. 2a shows a typical relationship of 3D parameters with the sampling interval for a grinding wheel surface. In Fig. 2a, the values of the parameters are normalised so that the value of the parameters at the smallest sampling interval is one. Similarly, the sampling intervals are normalised by dividing the sampling intervals by the value of S_{al} at the smallest interval. Fig. 2a reveals that the parameter S_{al} (the correlation length) is hardly affected by the sampling interval. Its value remains fairly constant until the sampling interval exceeds a certain value. The behaviour of S_{al} can be explained by the Wiener–Khinchin theorem, which states that the autocorrelation and the power spectrum are a pair of Fourier transforms

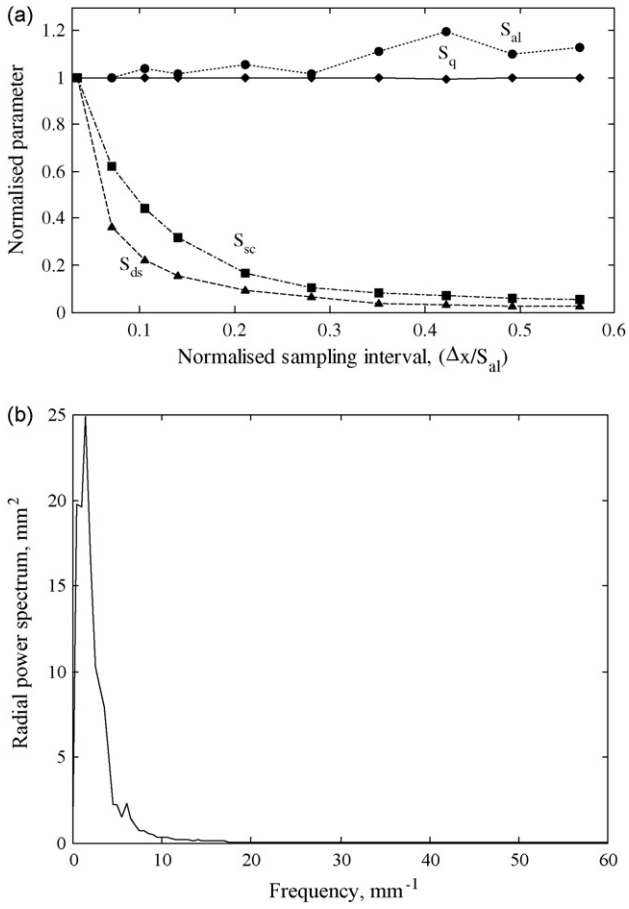

Fig. 2 – (a) 3D characterisation parameters of grinding wheels at various sampling intervals for B140N200V grinding wheel surface and (b) radial power spectrum of B140N200V grinding wheel surface.

(Papoulis, 1962). On the other hand, the power spectrum of the grinding wheel surface is dominated by only a few frequency components (Fig. 2b). Thus, S_{al} is affected by a few dominant frequency components in the spectrum. Until the sampling interval increases to some critical values these components are not affected, hence S_{al} remains unchanged. This correlation is further confirmed by the fact that the critical value, until which S_{al} is fairly constant, is approx. 0.3–0.5 as the requirement of the Nyquist sampling theorem (Nguyen and Bulter, 2005).

It can be noted that the value of S_{al} is slightly increased with the sampling interval in the range from 0.1 to 0.5. It can be explained by the fact that increasing the value of the sampling interval is equivalent to reducing the value of the low-pass filtering frequency. With an increased value of the sampling interval, more higher frequencies of the surface will be filtered out and folding back into the lower frequencies by the aliasing effect (Papoulis, 1962). With the value of the sampling interval higher than 0.5, the value of S_{al} will be fluctuated as most of the major frequencies of the surface are filtered out (Nguyen and Bulter, 2005).

As the abrasive grain is the major component of the grinding wheel, its distribution, size and shape will determine the

topography of the wheel. Consequently, it will reflect on the frequency components of the surface, and eventually on S_{al}. Thus, a sampling interval, based on S_{al} will better account for the varied distribution and size of abrasive grains in the grinding wheel.

An experiment was conducted to determine the optimal interval for counting abrasive grain. Samples of grinding wheels A80J8V (aluminium oxide, average grain size 226 μm), B120H200V (cubic boron nitride, average grain size 139 μm), and C120J8V (silicon carbide, average grain size 144 μm) and diamond pad conditioner A160 (diamond, average grain size 116 μm) were measured on the Talyscan 150 stylus system and observed in the JEOL5600 scanning electron microscope (SEM) system. The samples were marked so that the same area could be measured and observed on the stylus and SEM systems. The stylus speed was 0.5 mm/s and the sampling interval was 5 μm. For all the samples, the parameter S_{ds} was estimated at various sampling intervals. An abrasive grain was identified from the stylus image using the "eight nearest neighbour" definition. For the SEM images, abrasive grains were counted by visual inspection. Fig. 3 shows the topography of one sample obtained by the stylus and SEM systems.

Fig. 4 shows the relationship between the parameter S_{ds} and the sampling interval for various abrasive tools. The symbols ●,■, ▲, ♦ highlight the position of the counts of abrasive grains in relation with the sampling interval. The number of abrasive grains counted on the SEM images for the samples corresponds to the number of summits identified on the stylus images at the sampling interval $(0.27–0.35)S_{al}$, or

$$\frac{S_{al}}{4} \leq \Delta \leq \frac{S_{al}}{3} \tag{6}$$

Fig. 4 also displays the values of S_{ds} at the sampling intervals as recommended by Blunt and Ebdon (1996). These values are generally larger than the number of grains found on the SEM images while the chosen sampling intervals are approximately in the range $(0.2–0.3)S_{al}$. The resemblance between Eqs. (4) and (6) is clear and not coincident. Their similarity is obviously due to the correlation of S_{al} and an abrasive grain size. Compared to using the diameter of grains, S_{al} is a better criterion for selecting the optimal sampling interval as it accounts for the uneven distribution and the variability of grains.

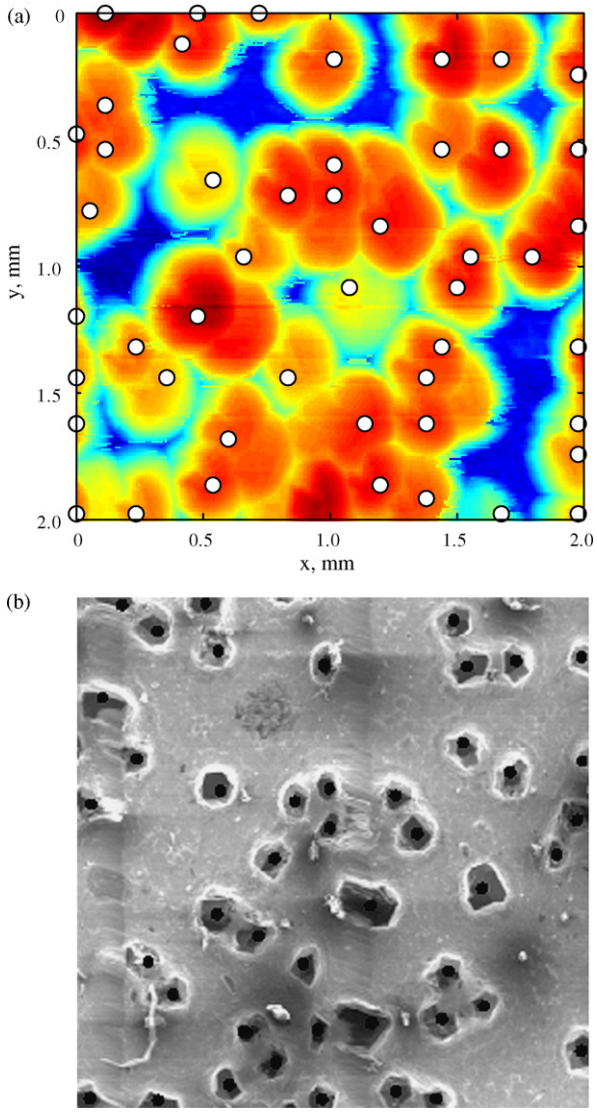

Fig. 3 – Topography of a diamond conditioning pad: (a) obtained by a stylus system; (b) obtained by SEM. The dot marks the position of the abrasive grain, found using the sampling interval of $0.33S_{al}$ (stylus) and visual inspection (SEM).

4. Experiment procedure

The relationship between the grinding wheel topography and its performance was studied using a 2^3 experimental design, in which the truing parameters were varied. The wheel performance was tested by grinding a workpiece of Inconel 718. Three replications of the experiment were conducted.

4.1. *Grinding conditions*

A high-speed surface grinding machine Okamoto 63DXNC equipped with a high-speed and high-power spindle was used for the investigation. The spindle system was balanced by an on-machine microbalancer. The amplitude of the wheel head vibration was adjusted to be less than 0.1 μm peak-to-peak at a maximum rotational speed of 5000 rpm. A 3-channel dynamometer Kistler 9265B was used to measure the grinding forces. Signals from the dynamometer were amplified by multi-channel amplifier Kistler 5019 before being captured using Labview 12-bit DAQ system. The grinding conditions are given in Table 1.

Table 1 – Grinding conditions

Grinding wheel velocity v_s (m/s)	50
Workpiece velocity v_w (m/s)	0.015
Depth of cut a (μm)	20
Transverse step w (mm)	3
Coolant	Water-soluble coolant
Grinding wheel	B140N200V

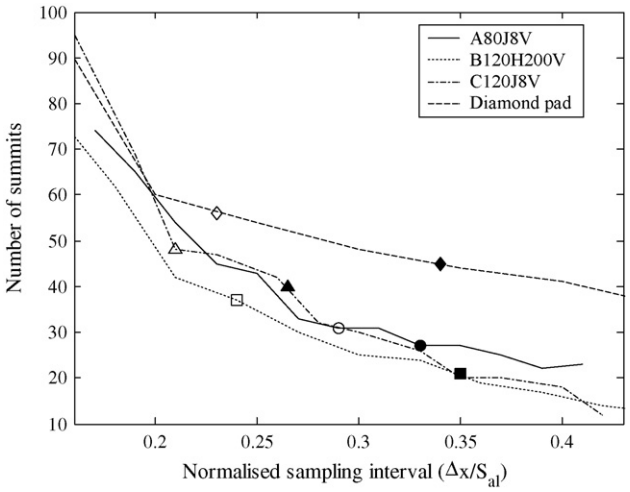

Fig. 4 – Number of summits at various intervals: symbols ●, ■, ▲, and ♦ mark the number of grains counted on SEM images for A80J8V, B120H200V, C120J8V, and diamond pad respectively. Symbols ○,□, △, and ◊ mark the number of summits at the sampling intervals chosen according to Blunt and Ebdon (1996).

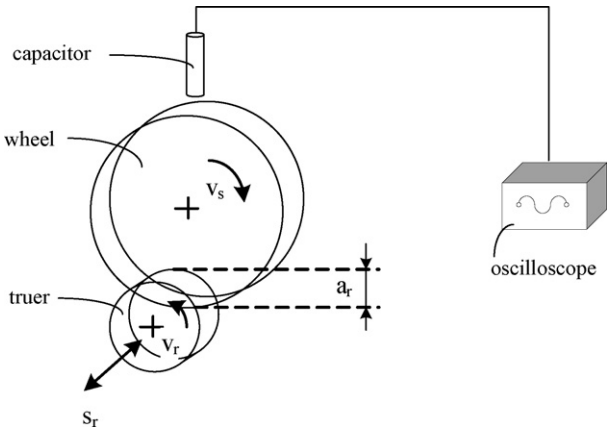

Fig. 5 – Truing operation.

4.2. *Truing and dressing conditions*

The truing operation was conducted in downcut mode (v_s/v_r = positive). A diagram of truing operations is given in Fig. 5. The truer velocity v_r, crossfeed s_r and truing depth a_r were varied according to a 2^3 factorial design.

Table 2 – A 2^3 factorial design for truing the grinding wheels

Run	Truer velocity (m/s)	Crossfeed (mm/rev)	Truing depth (μm)
1	10.5	0.3	30
2	10.5	0.3	10
3	10.5	0.1	30
4	10.5	0.1	10
5	6	0.3	30
6	6	0.3	10
7	6	0.1	30
8	6	0.1	10

Table 3 – Workpiece surface roughness S_q

Run	S_q		
	Replica 1	Replica 2	Replica 3
1	0.43	0.52	0.52
2	0.32	0.33	0.31
3	0.38	0.37	0.34
4	0.29	0.30	0.27
5	0.47	0.46	0.47
6	0.33	0.36	0.39
7	0.33	0.38	0.38
8	0.20	0.18	0.20

The wheel and truer velocities were chosen so that the speed ratios are 0.4 and 0.7, respectively. Although it is recommended that the wheel should be trued at its working speed, the grinding wheel speed in truing was limited to 1400 rpm due to the restricted speed of the truer. For truing, a rotary truer with SiC wheel C80M7V was used. The speed of the truer was controlled by a Eurotherm 601 variable speed drive. The wheel was trued until the run-out was less than 10 micron. The run-out of the wheel was checked using the capacitive sensing system Lion Precision DX405HA. The signal from the capacitive sensing system was recorded by the digital oscilloscope LeCroy 9300 series. After truing the wheel was dressed by plunge grinding into an abrasive stick A320 with a depth of 10–15 mm and at a plunge rate of approximate 150 mm/min. Table 2 summarises the truing conditions.

5. Results and discussion

The topography of the workpiece and the grinding wheels were obtained using the Talyscan 150 stylus system. The sampling interval for the workpiece topography was 5 μm; and for the grinding wheel topography was 15 μm. The sampling area

Table 4 – Analysis of variance for S_q of the workpiece

Source of variation	v_r	s_r	a_r	$v_r x\, s_r$	$v_r x\, a_r$	$s_r x\, a_r$	$v_r x\, s_r x\, a_r$	Error	Total
Estimate of effect	0.02	0.11	0.13	−0.01	−0.03	0.01	0.04		
Sum of squares	0.002	0.069	0.105	0.001	0.004	0.000	0.008	0.011	0.20
Degree of freedom	1	1	1	1	1	1	1	16	23
Mean-square	0.002	0.069	0.105	0.004	0.001	0.000	0.008	0.001	
F	2.65	103.83	157.74	0.75	6.63	0.38	12.41		
p-Value	0.12	0.00	0.00	0.40	0.02	0.55	0.00		

Table 5 – Grinding forces

Run	Tangential force (N)			Normal force (N)		
	Replica 1	Replica 2	Replica 3	Replica 1	Replica 2	Replica 3
1	4.59	4.28	4.40	11.55	12.50	11.34
2	4.84	4.39	4.38	13.46	12.86	11.33
3	4.10	4.45	4.93	11.58	12.64	12.84
4	4.90	4.59	4.38	12.53	11.39	10.81
5	4.63	5.07	4.89	13.78	13.12	12.31
6	5.51	5.18	5.88	14.98	14.10	14.61
7	4.43	4.93	5.07	14.09	14.98	14.98
8	5.90	5.02	4.87	15.53	15.07	15.11

Table 6 – Analysis of variance for tangential forces

Source of variation	v_r	s_r	a_r	$v_r x\, s_r$	$v_r x\, a_r$	$s_r x\, a_r$	$v_r x\, s_r x\, a_r$	Error	Total
Estimate of effect	−0.60	0.04	−0.34	−0.12	0.22	−0.05	0.06		
Sum of squares	2.13	0.01	0.69	0.08	0.28	0.01	0.02	1.88	5.10
Degree of freedom	1	1	1	1	1	1	1	16	23
Mean-square	2.13	0.01	0.69	0.08	0.28	0.01	0.02	0.12	
F	18.15	0.07	5.89	0.71	2.43	0.11	0.17		
p-Value	0.00	0.79	0.03	0.41	0.14	0.74	0.69		

Table 7 – Analysis of variance for normal forces

Source of variation	v_r	s_r	a_r	$v_r x\, s_r$	$v_r x\, a_r$	$s_r x\, a_r$	$v_r x\, s_r x\, a_r$	Error	Total
Estimate of effect	−2.32	−0.47	−0.51	0.68	0.52	−0.62	−0.15		
Sum of squares	32.34	1.32	1.54	2.75	1.61	2.29	0.13	7.77	49.74
Degree of freedom	1	1	1	1	1	1	1	16	23
Mean-square	32.34	1.32	1.54	2.75	1.61	2.29	0.13	0.49	
F	66.61	2.71	3.17	5.67	3.31	4.71	0.27		
p-Value	0.00	0.12	0.09	0.03	0.09	0.05	0.61		

for the grinding wheel and the workpiece was 3 mm × 3 mm and 2 mm × 2 mm, respectively. The grinding forces data captured by Labview were stored in ASCII format, and later processed using a MATLAB script. The values of the grinding forces were averaged from several grinding passes.

5.1. *Workpiece roughness*

The surface roughness S_q of the workpieces and their ANOVA result are shown in Tables 3 and 4. The ANOVA analysis for the workpiece roughness reveals that its roughness is strongly influenced by truer velocity, crossfeed and the truing depth in truing. Increasing the truer velocity, crossfeed or the truing depth will cause the workpiece surface to degrade. Among the parameters, the crossfeed and the truing depth display the strongest influence while the effect of the truer velocity is significant at the confidence level of 90%. Moreover, there were significant interaction effects between the truing speed and truing depth.

5.2. *Grinding forces*

The grinding forces and the corresponding ANOVA results are shown in Tables 5–7, respectively. The ANOVA analysis for the tangential forces highlights the considerable effects on the force by the truer velocity and truing depth. The tangential force rises when the truer velocity or the truing depth falls. On the other hand, changing the value of crossfeed seems not to affect the tangential force. Meanwhile, the ANOVA analysis for the normal force indicates that all the parameters of the truing mode can influence the force at the significant level less than 10%. Among the factors, the truer velocity and truing depth display the largest effect. Similarly to the tangential force, reducing the truer velocity, crossfeed and the truing depth makes the normal force drop. Furthermore, the interaction effects between the truing factors on the normal force are significant at the level of 0.1 while such interaction is negligible for the tangential force.

Table 8 – Average surface roughness S_q of the grinding wheels (μm)

Run	Replica 1	Replica 2	Replica 3
1	13.61	15.44	13.82
2	13.20	13.07	14.08
3	11.44	11.50	10.48
4	14.07	12.55	13.71
5	13.86	15.27	12.76
6	9.93	10.83	9.09
7	13.20	14.25	14.59
8	10.63	10.69	9.31

Table 9 – Analysis of variance for S_q of the grinding wheels

Source of variation	v_r	s_r	a_r	$v_r x s_r$	$v_r x a_r$	$s_r x a_r$	$v_r x s_r x a_r$	Error	Total
Estimate of effect	1.05	0.71	1.59	0.87	−2.32	0.84	0.73		
Sum of squares	6.59	3.03	15.17	4.50	32.23	4.22	3.23	11.52	80.49
Degree of freedom	1	1	1	1	1	1	1	16	23
Mean-square	6.59	3.03	15.17	4.50	32.23	4.22	3.23	0.72	
F	9.16	4.21	21.07	6.25	44.78	5.87	4.49		
p-Value	0.01	0.06	0.00	0.02	0.00	0.03	0.05		

Table 10 – Average density of summits S_{ds} of the grinding wheels (mm^{-2})

Run	Replica 1	Replica 2	Replica 3
1	22.22	14.85	23.07
2	23.52	21.71	20.24
3	27.89	26.13	26.64
4	20.01	21.99	20.97
5	23.69	20.97	25.28
6	27.21	27.83	31.52
7	26.07	18.71	17.12
8	26.76	29.59	34.58

Table 12 – Average density of summits S_{sc} of the grinding wheels (mm^{-1})

Run	Replica 1	Replica 2	Replica 3
1	0.005	0.004	0.005
2	0.004	0.004	0.005
3	0.004	0.004	0.004
4	0.004	0.005	0.004
5	0.005	0.004	0.005
6	0.005	0.005	0.004
7	0.005	0.004	0.004
8	0.004	0.005	0.005

5.3. *Grinding wheel topography*

The 3D parameters of the grinding wheel topographies and their corresponding ANOVA results are presented respectively in Tables 8–13. For the evaluation of the grinding wheel topography, the grinding wheel topography was obtained at two separate locations. The values of the surface characterisation parameters were averaged from the two samples for each experimental run. One topographical sample of the grinding wheel is shown in Fig. 6.

The coarseness of the grinding wheel can be evaluated through the root-mean-square parameter S_q (Table 8). It is evident from the ANOVA analysis that the truing parameters have similar effects on the grinding wheel topography (Table 9) as on the workpiece surfaces (Table 4). All truing factors exert considerable influence on the wheel roughness. Raising the truing velocity, the crossfeed and the depth of cut will make the wheel rougher or, in other words coarser. Furthermore all the interaction effects between the factors are significant at the level of 0.05.

For the characterisation of the abrasive grains, the parameters density of summits S_{ds} (Table 10) and summits curvature S_{sc} (Table 12) are used as the indicator of the abrasive grain density and sharpness. In order to estimate the parameters S_{ds} and S_{sc}, the sampling interval for the grinding wheel topography was selected as 45 μm according to Eq. (6). The sampling interval was estimated using the averaged value of the correlation lengths of all the sampled wheel topography S_{al} = 170 μm.

For the density of summits S_{ds} of the grinding wheels, the augmentation of the truer velocity and truing depth will cause the drop of S_{ds} while the crossfeed does not have significant

Table 11 – Analysis of variance for S_{ds} of the grinding wheels

Source of variation	v_r	s_r	a_r	$v_r x s_r$	$v_r x a_r$	$s_r x a_r$	$v_r x s_r x a_r$	Error	Total
Estimate of effect	−3.34	−1.20	−2.77	−1.81	4.83	−0.88	−2.95		
Sum of squares	66.92	8.57	46.13	19.64	140.10	4.68	52.31	147.26	485.60
Degree of freedom	1	1	1	1	1	1	1	16	23
Mean-square	66.92	8.57	46.13	19.64	140.10	4.68	52.31	9.20	
F	7.27	0.93	5.01	2.13	15.22	0.51	5.68		
p-Value	0.02	0.35	0.04	0.16	0.00	0.49	0.03		

Table 13 – Analysis of variance for S_{sc} of the grinding wheels

Source of variation	v_r	s_r	a_r	$v_r x s_r$	$v_r x a_r$	$s_r x a_r$	$v_r x s_r x a_r$	Error	Total
Estimate of effect	−3.3E−4	0	−8.3E−5	8.3E−5	0	1.7E−4	−8.3E−5		
Sum of squares	6.7E−7	0	4.2E−8	4.2E−8	0	1.7E−7	4.2E−8	3.0E−6	4.0E−6
Degree of freedom	1	1	1	1	1	1	1	16	23
Mean-square	6.7E−7	0	4.2E−8	4.2E−8	0	1.7E−7	4.2E−8	1.9E−7	
F	3.56	0.00	0.22	0.22	0.00	0.89	0.22		
p-Value	0.08	1.00	0.64	0.64	1.00	0.36	0.64		

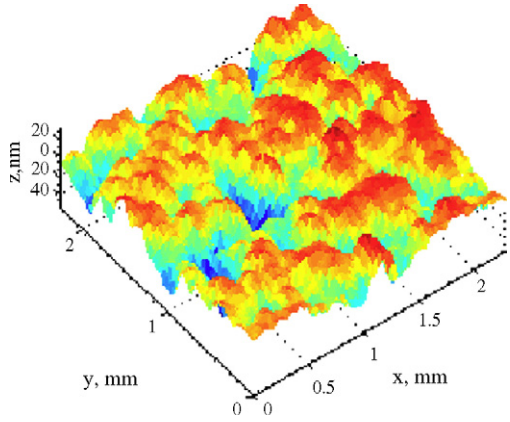

Fig. 6 – Topographical sample of the grinding wheel.

effect on the parameter. The interaction effects of the truing factors are also significant on S_{ds} at the confidence level of 90% (Table 11). In contrast, S_{sc} is affected only by the truer velocity; increasing the truing velocity will make S_{sc} decrease. The other factors show no influence at large levels of significance (Table 13).

5.4. *Correlation between the grinding wheel and workpiece surface parameters*

Table 14 displays the effects of the truing factors on the grinding wheel topography and the grinding performance. It is clear from the table that there is a similarity between the effect of truing factors on the grinding performance and the 3D characterisation parameters of the wheel topographies. The surface roughness of the workpiece, the normal force, as well as the parameter S_q of the grinding surface are affected by all three truing factors. On the other hand, the normal force and the parameter S_{ds} are only influenced by the truer velocity and depth of cut. This similarity of the effects on the grinding wheel topography and the grinding performance suggests there is correlation between the parameters.

The impact of the truing factors on the workpiece surface roughness can be explained using the grinding wheel topographical parameters. Increasing the truer velocity, crossfeed and depth of cut would coarsen the grinding wheel, evident by the increased S_q value of the grinding wheel topography, which in turn induces a rougher workpiece surface (Fig. 7a). The degradation of the workpiece quality is also due to the decrease of the number of active abrasive grains, according to

Table 14 – Effects of the truing parameters on the grinding wheel topography and grinding performance

Parameters	Truer velocity	Crossfeed	Depth of cut
S_q (workpiece)	×	×	×
Tangential force	×		×
Normal force	×	×	×
S_q (wheel)	×	×	×
S_{ds}	×		×
S_{sc}	×		

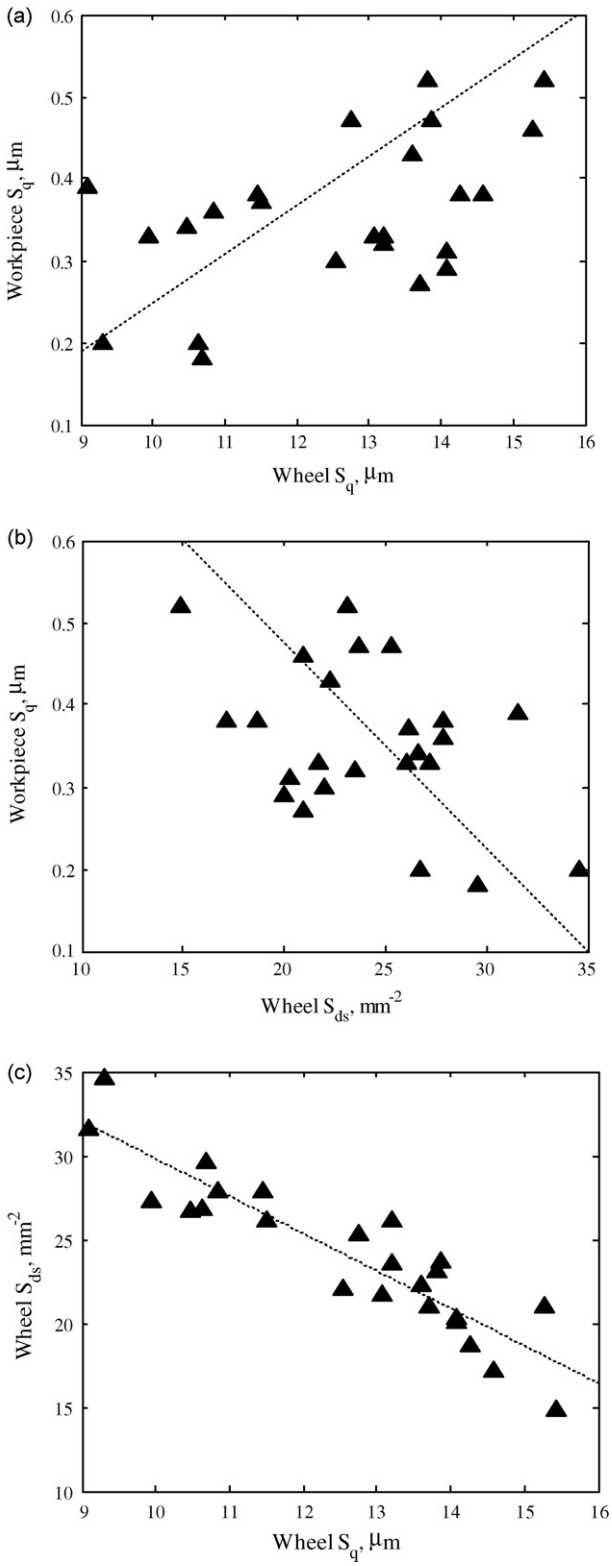

Fig. 7 – Correlation between the parameters: (a) S_q of the workpiece and S_q of the grinding wheel; (b) S_q of the workpiece and S_{ds} of the grinding wheel; (c) correlation between the parameters S_{ds} and S_q of the grinding wheel.

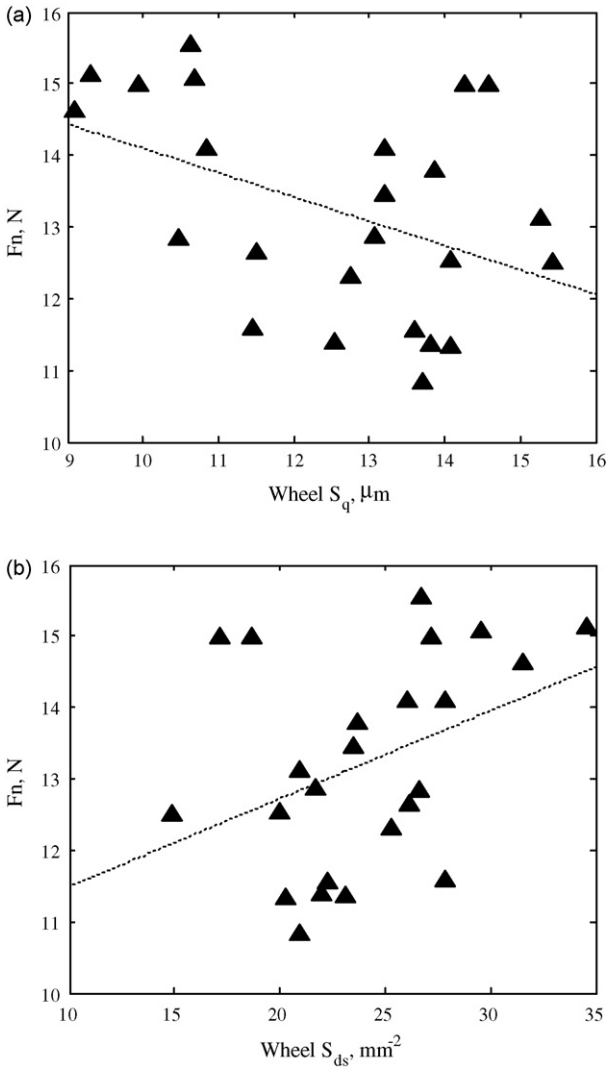

Fig. 8 – Correlation between the normal force Fz and the parameters: (a) S_q; (b) S_{ds} of the grinding wheel.

the parameters S_{ds} (Fig. 7b). The correlation of the workpiece S_q with the grinding wheel S_q and S_{ds} is however not independent as there is a linear relationship between the values S_q and S_{ds} of the grinding wheel as suggested by Fig. 7c.

Table 15 – *p*-Value for the grinding wheel parameters at various sampling intervals

Parameters	Sampling interval (μm)	Truer velocity	Crossfeed	Truing depth
S_q	30	0.01	0.06	0
	45	0.01	0.06	0
	60	0.01	0.06	0
S_{ds}	30	0.02	0.79	0.04
	45	0.02	0.35	0.04
	60	0.04	0.01	0.01
S_{sc}	30	0.08	0.08	0.27
	45	0.08	1.00	0.64
	60	1.00	0.51	1.00

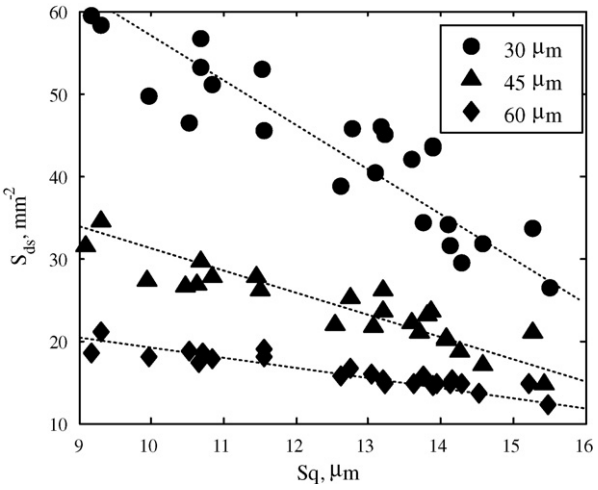

Fig. 9 – Correlation between the parameters S_q and S_{ds} of the grinding wheel at sampling interval 30, 45 and 60 μm.

Similarly, the influence of the truing parameters on the grinding forces can be explained by the behaviour of the parameters S_{ds} and S_{sc}. The reduction of S_{ds} at larger truer velocities, crossfeeds and truing depths suggests a smaller number of active abrasive grains on the grinding wheel, thus, lowering the grinding forces. Moreover, the larger values of the truing speed would reduce S_{sc}, meaning lower sharpness of the abrasive grains. The combination of the reduced number of the abrasive grain and the sharpness due to the higher truing speed thus makes truing speed the most influential factor on the grinding force. Fig. 8 shows the correlation between the normal force and the parameter S_q and S_{ds} of the grinding wheel. Although the linear equation can be fitted to the data, the deviation of some data points hints that the grinding forces could be affected not only by the abrasive grain density but also by other factors.

It should be noted that the choice of the sampling interval could affect the ANOVA results, as the parameters S_{ds} and S_{sc} are strongly dependent on the value of the sampling interval. Table 15 displays the *p*-values of the parameters S_q, S_{ds} and S_{sc} at the sampling interval 30, 45 and 60 μm, which satisfy the following equation:

$$30 < \frac{S_{al}}{4} < 45 < \frac{S_{al}}{3} < 60 \quad (7)$$

Table 15 reveals that *p*-values for the parameter S_q are very consistent over the studied range of sampling intervals. On the other hand, the *p*-value for the parameters S_{ds} and S_{sc} are very sensitive to the used sampling interval. At the smaller value of the sampling interval, the truing factors would have more significant effect on S_{sc}; while at the larger sampling interval, S_{ds} is considerably influenced by all factors. Thus, care should be taken in choosing the sampling interval value for estimating S_{ds} and S_{sc}. A smaller value of the sampling interval would correlate S_{ds} and S_{sc} to random components on the grinding topography while a larger value would omit the essential components of the abrasive grain. However, the linear relationship between S_q and S_{ds} is still maintained despite the variation of

S_{ds} as shown in Fig. 9, which suggests that S_q is a more robust parameter for characterising grinding wheel topography.

6. Conclusions

It has been shown that the characteristics of the grinding wheel topography as well as its correlation with the grinding performance can be quantified in terms of the three-dimensional surface characterisation parameters. The parameters S_{ds}, S_{sc}, and S_q can be used as the density of abrasive grains, the sharpness of abrasive grains, and the coarseness of the wheel. Among the parameters, the root-mean-square S_q is rather robust for the characterisation purpose. However, care should be taken in choosing the sampling interval so that the parameters will reflect the components under consideration. The optimal sampling interval should be based on the correlation length in order to account for the non-uniform distribution of grains.

REFERENCES

American Society of Mechanical Engineers, ASME B64.1-1995 Surface texture: surface roughness, waviness, lay, 1995.

Blunt, L., Ebdon, S., 1996. The application of three-dimensional surface measurement techniques to characterizing grinding wheel topography. Int. J. Machine Tools Manuf. 36 (11), 1207–1226.

Brinksmeier, E., Cinar, M., 1995. Characterisation of dressing processes by determination of collision number of the abrasive grits. Ann. CIRP 44 (1), 299–304.

Butler, D.L., Blunt, L.A., See, B.K., Webster, J.A., Stout, K.J., 2002. The characterisation of grinding wheels using 3D surface measurement techniques. J. Mater. Process. Technol. 127 (2), 234–237.

Higuchi, M., Yano, A., Yamamoto, N., Adachi, T., Yamashita, K., 1994. Quantitative analysis grain using fractal geometry. Int. J. Jpn. Soc. Prec. Eng. 28 (3), 227–228.

Liao, T.W., 1995. Fractal and DDS characterization of diamond wheel profiles. J. Mater. Process. Technol. 53 (3–4), 567–581.

Malkin, S., 1998. Grinding Technology. Ellis Horwood, Chichester.

Nakajima, T., 1978. A new standard for proper selection of grinding wheels in plunge grinding operation. Ann. CIRP 27 (1), 249–253.

Nguyen, A.T., Bulter, D.L., 2005. Correlation-length-based sampling conditions for various engineering surfaces. Meas. Sci. Technol. 16, 1813–1822.

Papoulis, A., 1962. The Fourier Integral and Its Applications. McGraw-Hill, New York.

Stout, K.J., Sullivan, P.J., Dong, W.P., Mainsah, E., Luo, N., Mathia, T., Zahouani, H., 1993. The Development of Methods for the Characterisation of Roughness in Three Dimensions. EC, Luxembourg.

Tonshoff, H.K., Karpuschewski, B., Andrae, P., Turich, A., 1998. Grinding performance of superhard abrasive wheels—final report concerning CIRP co-operative work in STC "G". Ann. CIRP 47 (2), 723–732.

Verkerk, J., 1977. Final report concerning CIRP cooperative work on the characterization of grinding wheel topography. Ann. CIRP 26 (2), 385–395.